LUND UNIVERSITY

Equilibrium simulation of trp-cage in the presence of protein crowders.

Bille, Anna; Linse, Björn; Mohanty, Sandipan; Irbäck, Anders

Published in:
Journal of Chemical Physics

DOI:
10.1063/1.4934997

2015

Link to publication

Citation for published version (APA):
Bille, A., Linse, B., Mohanty, S., & Irbäck, A. (2015). Equilibrium simulation of trp-cage in the presence of protein crowders. *Journal of Chemical Physics*, *143*(17), Article 175102. https://doi.org/10.1063/1.4934997

Total number of authors:
4

General rights
Unless other specific re-use rights are stated the following general rights apply:
Copyright and moral rights for the publications made accessible in the public portal are retained by the authors and/or other copyright owners and it is a condition of accessing publications that users recognise and abide by the legal requirements associated with these rights.
• Users may download and print one copy of any publication from the public portal for the purpose of private study or research.
• You may not further distribute the material or use it for any profit-making activity or commercial gain
• You may freely distribute the URL identifying the publication in the public portal

Read more about Creative commons licenses: https://creativecommons.org/licenses/

Take down policy
If you believe that this document breaches copyright please contact us providing details, and we will remove access to the work immediately and investigate your claim.

LUND UNIVERSITY

PO Box 117
221 00 Lund
+46 46-222 00 00

AIP | The Journal of Chemical Physics

Equilibrium simulation of trp-cage in the presence of protein crowders

Anna Bille, Björn Linse, Sandipan Mohanty, and Anders Irbäck

Citation: The Journal of Chemical Physics **143**, 175102 (2015); doi: 10.1063/1.4934997
View online: http://dx.doi.org/10.1063/1.4934997
View Table of Contents: http://scitation.aip.org/content/aip/journal/jcp/143/17?ver=pdfcov
Published by the AIP Publishing

Articles you may be interested in

Sampling the equilibrium kinetic network of Trp-cage in explicit solvent
J. Chem. Phys. **140**, 195102 (2014); 10.1063/1.4874299

Global motions exhibited by proteins in micro- to milliseconds simulations concur with anisotropic network model predictions
J. Chem. Phys. **139**, 121912 (2013); 10.1063/1.4816375

Folding dynamics of Trp-cage in the presence of chemical interference and macromolecular crowding. I
J. Chem. Phys. **135**, 175101 (2011); 10.1063/1.3656691

Kinetics and mechanism of the unfolding native-to-loop transition of Trp-cage in explicit solvent via optimized forward flux sampling simulations
J. Chem. Phys. **133**, 105103 (2010); 10.1063/1.3474803

Energy landscape paving simulations of the trp-cage protein
J. Chem. Phys. **122**, 194711 (2005); 10.1063/1.1899149

This article is copyrighted as indicated in the article. Reuse of AIP content is subject to the terms at: http://scitation.aip.org/termsconditions. Downloaded to IP: 130.235.184.47 On: Tue, 08 Dec 2015 22:06:58

THE JOURNAL OF CHEMICAL PHYSICS **143**, 175102 (2015)

Equilibrium simulation of trp-cage in the presence of protein crowders

Anna Bille,[1,a)] Björn Linse,[1,b)] Sandipan Mohanty,[2,c)] and Anders Irbäck[1,d)]
[1]*Computational Biology and Biological Physics, Department of Astronomy and Theoretical Physics, Lund University, Sölvegatan 14A, SE-223 62 Lund, Sweden*
[2]*Institute for Advanced Simulation, Jülich Supercomputing Centre, Forschungszentrum Jülich, D-52425 Jülich, Germany*

(Received 18 August 2015; accepted 19 October 2015; published online 4 November 2015)

While steric crowders tend to stabilize globular proteins, it has been found that protein crowders can have an either stabilizing or destabilizing effect, where a destabilization may arise from nonspecific attractive interactions between the test protein and the crowders. Here, we use Monte Carlo replica-exchange methods to explore the equilibrium behavior of the miniprotein trp-cage in the presence of protein crowders. Our results suggest that the surrounding crowders prevent trp-cage from adopting its global native fold, while giving rise to a stabilization of its main secondary-structure element, an α-helix. With the crowding agent used (bovine pancreatic trypsin inhibitor), the trp-cage–crowder interactions are found to be specific, involving a few key residues, most of which are prolines. The effects of these crowders are contrasted with those of hard-sphere crowders. © *2015 AIP Publishing LLC.* [http://dx.doi.org/10.1063/1.4934997]

I. INTRODUCTION

In their natural environment, proteins are subject to crowding and confinement. How these factors influence protein-protein interactions and biomolecular processes such as folding, binding, and aggregation is a topic attracting increasing interest.[1–5] It is well established that excluded-volume interactions with crowder particles can have a significant stabilizing effect on globular proteins, as demonstrated by experiments with synthetic crowding agents such as Ficoll or dextran.[6] Today, experiments are increasingly often performed under more realistic crowding conditions, using concentrated protein solutions[7–10] or cells.[9,11–16] In these systems, it has been shown that other interactions may dominate over the steric repulsions and lead to a net destabilization of globular proteins.[7–9,12–14,16] For a fundamental understanding of these effects, there is a need for computational approaches that permit the simulation of folding/unfolding equilibria in the presence of complex biomolecular crowding agents.

In this article, we present a computational study of the folding thermodynamics of the 20-residue trp-cage[17] in the presence of protein crowders, using Monte Carlo (MC) methods and an all-atom protein representation with an implicit solvent force field.[18,19] As crowding agent, we pick the 58-residue bovine pancreatic trypsin inhibitor (BPTI), which was used in recent experiments on the disordered N protein of bacteriophage λ.[10] We model the BPTI molecules in full atomistic detail but assume them to stay folded with restricted internal dynamics. For comparison, we also perform simulations with simple hard-sphere crowders. The results obtained with BPTI and hard-sphere crowders are contrasted with data from reference simulations of trp-cage without crowders.[19]

Under dilute conditions, trp-cage is known from experiments to fold in a cooperative manner to a compact native state.[17] This property along with its convenient size and a folding time of only a few μs[20] has made trp-cage a widely used model system for protein folding simulations.[21–31] Its small size and fast folding also indicate that the native free-energy minimum is shallow, which in turn suggests that trp-cage might be sensitive to macromolecular crowding.

Since simulating proteins in crowded environments is computationally very challenging, coarse-grained approaches have been used to obtain valuable insights.[32–38] In many cases, the crowders have been modeled as hard spheres. To enable more detailed simulations, a post-processing alternative to direct simulation has been developed.[39–41] In this approach, one first produces a conformational ensemble for the test protein under crowder-free conditions, which is subsequently reweighted by insertion into separately generated crowder configurations. This procedure assumes that the conformational ensemble relevant under crowded conditions is not too different from that under dilute conditions. Although this procedure has been successfully tested on specific systems,[42] the general validity of the above mentioned assumption is not obvious. Recently, pioneering direct simulations, avoiding this assumption, were reported by Feig, Sugita, and coworkers.[8,43,44] These authors performed molecular dynamics simulations of some small proteins, including trp-cage,[44] in the presence of protein crowders, focusing on local stability properties. In the trp-cage study, protein GB1 served as the crowding agent.

In the present work, we use MC-based replica-exchange simulations to explore the global folding thermodynamics of trp-cage in the presence of BPTI crowders. Our results can be compared with those from the previous study with protein GB1 crowders.[44] BPTI and protein GB1 are similar in size, but differ, for instance, in terms of net charge.

a)Electronic mail: anna.bille@thep.lu.se
b)Electronic mail: bjorn.linse@gmail.com
c)Electronic mail: s.mohanty@fz-juelich.de
d)Electronic mail: anders@thep.lu.se

 © 2015 AIP Publishing LLC

This article is copyrighted as indicated in the article. Reuse of AIP content is subject to the terms at: http://scitation.aip.org/termsconditions. Downloaded to IP: 130.235.184.47 On: Tue, 08 Dec 2015 22:06:58

II. METHODS

A. Model

We simulate the folding thermodynamics of trp-cage under three sets of conditions: (i) with BPTI crowders, (ii) with hard-sphere crowders, and (iii) without crowders. All simulations are performed using an all-atom protein representation with fixed bond lengths and bond angles and an implicit solvent force field.[19] A detailed description of the interaction potential can be found elsewhere.[19] In brief, the potential consists of four main terms, $E = E_{\rm loc} + E_{\rm ev} + E_{\rm hb} + E_{\rm sc}$. The first ($E_{\rm loc}$) represents local interactions between atoms separated by only a few covalent bonds. The other terms are non-local and represent excluded-volume effects ($E_{\rm ev}$), hydrogen bonding ($E_{\rm hb}$), and residue-specific interactions between pairs of sidechains, based on hydrophobicity and charge ($E_{\rm sc}$). The $E_{\rm ev}$, $E_{\rm hb}$, and $E_{\rm sc}$ energies contain both intra- and intermolecular terms. Intermolecular interaction terms have the same form and strength as intramolecular ones. The potential was parameterized through folding thermodynamics studies for a structurally diverse set of peptides and small proteins, which included trp-cage.[19] This computational model has not previously been used for crowding simulations but has been applied to study peptide aggregation[45,46] and the conformational ensembles sampled by several proteins with >90 residues.[47–50]

In our simulations with BPTI crowders, we include all atoms of the BPTI molecules. However, for computational tractability, we assume these molecules to stay folded, with a fixed backbone and thus with sidechain torsion angles as their only degrees of freedom. This approximation is reasonable, as the thermal stability of BPTI is high.[51] The test protein, trp-cage, is modeled without these constraints and thus free to fold and unfold in the simulations. The assumed backbone conformation of BPTI is a model approximation of the crystal structure (PDB ID 4PTI), derived by Monte Carlo with minimization. The structure was selected for both low energy and high similarity to the crystal structure. Its root-mean-square deviation (RMSD) from the crystal structure (calculated over backbone and C^β atoms) was approximately 1 Å.

The three disulfide bonds present in the BPTI molecule are modeled with geometric restraints. Each disulfide bond is described using four harmonic distance restraints, involving the S and C^β atoms of the two cysteins. Equilibrium distances for the harmonic potentials are extracted from the crystal structure.

In our second set of crowding simulations, we use abstract non-overlapping spherical crowders. The interaction energy u between a trp-cage atom with radius σ_i and a spherical crowder with radius $\sigma_{\rm C}$, at center-to-center distance r, is $u = 0$ if $r > \sigma_i + \sigma_{\rm C}$, and $u = \infty$ otherwise. The crowder radius is set to either $\sigma_{\rm C} = 12.5$ Å or $\sigma_{\rm C} = 17.2$ Å. The small radius yields a volume similar to that occupied by a BPTI molecule. The large crowders have a diameter roughly similar to the maximum diameter of BPTI. Our simulations with spherical crowders, with purely steric interactions, serve as a reference, which is useful in interpreting the results obtained with BPTI crowders. In the latter system, the intermolecular interactions are a complex mixture of attractive and repulsive terms, representing excluded-volume effects, hydrogen bonding, hydrophobic attraction, and charge-charge interaction.

B. MC details

We simulate these different systems using MC replica-exchange techniques,[52] with 16 different temperatures geometrically distributed between 273 K and 373 K. For the system with BPTI crowders, we do not report any results at the three lowest simulated temperatures, due to poor mobility of these temperatures between replicas. The statistical robustness of data over the remaining temperature interval (290 K–373 K) was confirmed by an independent replica-exchange simulation with 290 K as the lowest temperature.

In all our crowding simulations, the system consists of one trp-cage molecule and eight crowder molecules or particles, enclosed in a periodic box with side length 95 Å. Note that the periodicity does not cause any ambiguities in our energy calculations, since all interactions have a cutoff distance that is short compared to the box length. The volume fraction occupied by BPTI crowders is about 7%, and the BPTI density is ~100 mg/ml. This value is lower than estimated macromolecule densities in cells (~300–400 mg/ml),[53] but sufficiently high for noticeable crowding effects to occur in the simulations, as will be seen below. The volume fractions occupied by our small ($\sigma_{\rm C} = 12.5$ Å) and large ($\sigma_{\rm C} = 17.2$ Å) spherical crowders are 7% and 20%, respectively.

Our MC move set is as described previously.[46] The simulations are started with trp-cage in a random initial conformation and the crowders placed in the corners of a virtual cube, which is smaller than the simulation box (Fig. 1). All our calculations are performed using the program package PROFASI.[18] Recent

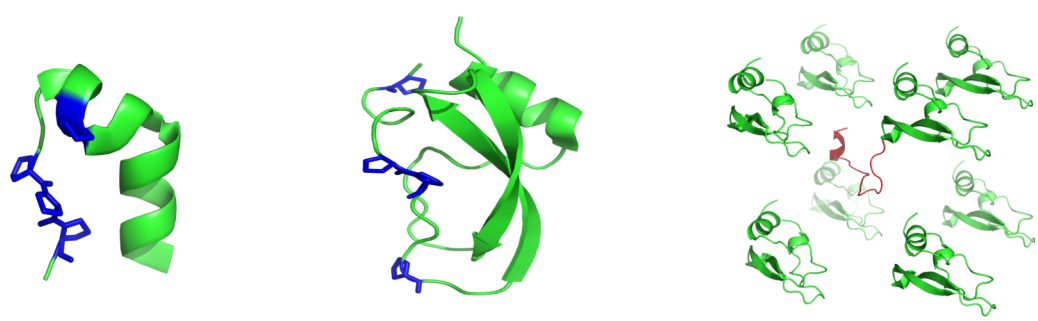

FIG. 1. Schematic illustrations of (left) the native trp-cage structure (PDB ID 1L2Y), (center) the native BPTI structure (PDB ID 4PTI), and (right) the initial state for the simulations of trp-cage (red) with BPTI crowders (green). Blue color indicates proline (residues 12 and 17–19 in trp-cage; residues 2, 8, 9, and 13 in BPTI).

This article is copyrighted as indicated in the article. Reuse of AIP content is subject to the terms at: http://scitation.aip.org/termsconditions. Downloaded to IP: 130.235.184.47 On: Tue, 08 Dec 2015 22:06:58

optimizations in PROFASI including a redesign targeting vector and thread parallelization reduce the overall computing time by an order of magnitude.

Of our systems, by far the most computationally challenging one is that with BPTI crowders. Our simulation of that system comprised 10^7 MC sweeps for each of the 16 replicas, where one sweep consists of $N_{\mathrm{dof}} = 1155$ attempted elementary MC updates, N_{dof} being the total number of degrees of freedom under the simulation conditions.

C. Analysis

In the simulations, we monitor several different structural properties of trp-cage. The fraction of α-helical residues, H, is computed using STRIDE secondary-structure assignments.[54] The extension of the protein chain is assessed using both the radius of gyration, R_{g}, calculated over all non-hydrogen atoms, and the C^{α}-C^{α} distance between the two end residues, R_{ee}. The end-to-end distance can be used to detect non-native conformations where the N-terminal α-helix is intact but not packed against the C-terminal tail (Fig. 1). As an overall measure of nativeness, we use the backbone RMSD from the NMR structure (PDB ID 1L2Y), Δ, calculated over residues 2–19. The two end residues are flexible and therefore omitted in the RMSD calculation.

In addition, we measure residue-pair contact frequencies. Two residues are defined to be in contact if their C^{α} atoms are within 6 Å of each other. In a given trp-cage–BPTI configuration, we count the number of contacts that residue i in trp-cage forms with residue j in any of the BPTI chains, for all i and j. These numbers are denoted by n_{ij}^{tc}. Similarly, n_{ij}^{cc} is defined as the number of contacts that residue i in a given BPTI molecule forms with residue j in any of the other BPTIs. The average matrices n_{ij}^{tc} and n_{ij}^{cc} are visualized in contact maps.

III. RESULTS

Using the above methods, we simulate systems consisting of one trp-cage and eight BPTI or spherical crowders. Our analysis consists of two parts. First, we determine the folding thermodynamics of trp-cage in the different environments. Second, by constructing residue-pair contact maps, we identify the key modes of intermolecular interaction in the trp-cage–BPTI system.

A. Folding thermodynamics of trp-cage

The response of a protein to the presence of surrounding crowders generally involves both energetic and entropic factors, whose relative importance depends on temperature. We therefore analyze the folding properties of trp-cage over a wide range of temperatures in the different environments. The results of this analysis are summarized in Fig. 2, which shows the temperature-dependence of the helix content (H), the radius of gyration (R_{g}), the RMSD from the NMR structure (Δ), and the end-to-end distance (R_{ee}).

We first discuss the results obtained with spherical crowders, with purely steric interactions. As expected, these crowders cause a compaction of trp-cage (Figs. 2(b) and 2(d)). This effect, entropic in nature, is negligible at low temperatures

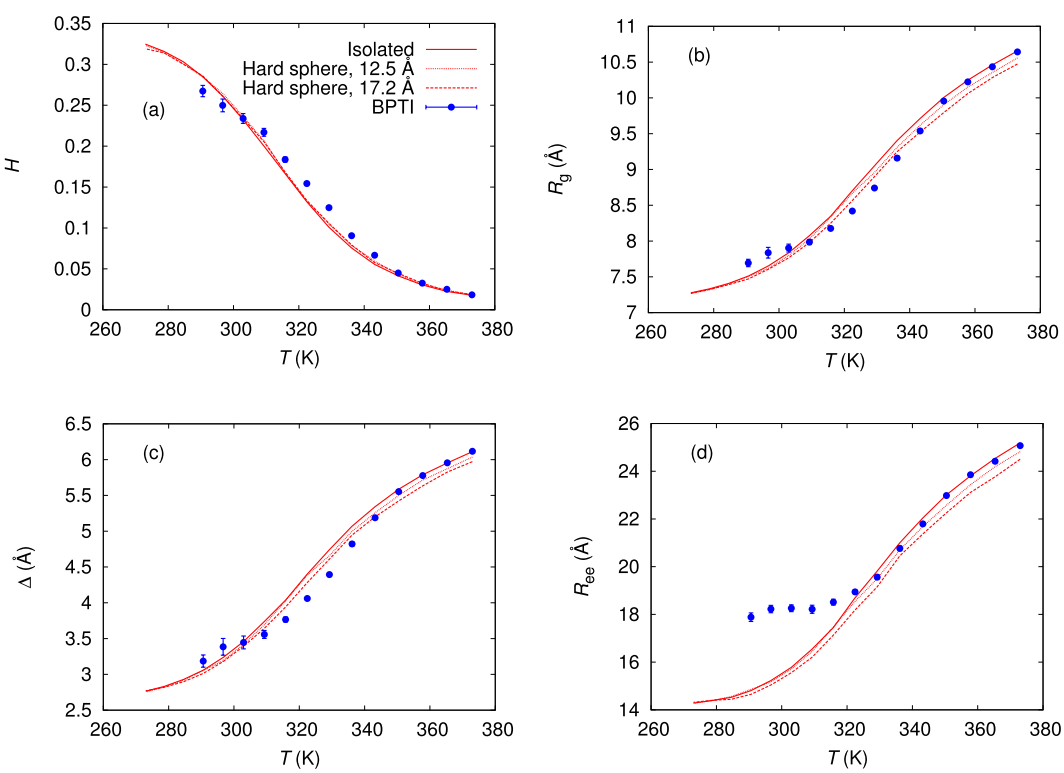

FIG. 2. Folding thermodynamics of trp-cage without crowders (red line), with small/large spherical crowders (red dots/dashes), and with BPTI crowders (blue symbols). With no or spherical crowders, the statistical uncertainties are small and, for clarity, omitted. The quantities shown are (a) the helix content (H), (b) the radius of gyration (R_{g}), (c) the backbone RMSD (Δ), and (d) the end-to-end distance (R_{ee}).

This article is copyrighted as indicated in the article. Reuse of AIP content is subject to the terms at: http://scitation.aip.org/termsconditions. Downloaded to IP: 130.235.184.47 On: Tue, 08 Dec 2015 22:06:58

but noticeable at high temperatures. The degree of compaction becomes larger as the crowder radius is increased. The compaction leads to a reduced RMSD (Fig. 2(c)) and therefore to an apparent stabilization of trp-cage. However, in isolation, the small trp-cage does not behave as an ideal two-state protein in our model, although simulated melting curves can be well described in terms of a simple two-state picture.[19] Hence, one might expect crowding effects not to be uniform, but depend on the property studied. This is indeed the case in our simulations, as illustrated by the data for the helix content (Fig. 2(a)). In contrast to the radius of gyration and the end-to-end distance, the helix content is left virtually unchanged in the presence of the crowders.

We now turn to the simulations with BPTI crowders, which influence trp-cage via both repulsive and attractive interactions. The latter ones compete with the attractive intramolecular interactions driving the folding of the test protein. In fact, in our simulations, their impact is sufficiently strong to cause a distortion of the native form of trp-cage at low temperatures (Fig. 2). Effects of the BPTI crowders can also be seen at intermediate temperatures, 300 K $\lesssim T \lesssim$ 340 K, where the melting temperature of trp-cage (~315 K) is situated.[17] At these temperatures, the BPTI crowders cause an apparent stabilization of trp-cage (Fig. 2(c)). The helix content increases and the radius of gyration decreases in the presence of the crowders (Figs. 2(a) and 2(b)). A more detailed residue-level secondary-structure analysis confirms that this increase in overall helix content is due to a stabilization of native α-helix, spanning residues 2–9, rather than to formation of non-native α-helix structure (Fig. 3). With spherical crowders, the residue-specific α-helix probabilities are, by contrast, essentially identical to those for trp-cage in isolation (Fig. 3).

Comparison to the results obtained with spherical crowders shows that the BPTI-induced apparent stabilization of trp-cage at intermediate temperatures cannot be due to steric interactions. Attractive interactions, on the other hand, might, at first glance, be expected to have a destabilizing role, by favoring potentially more interaction-prone unfolded forms of the test protein over the native form. However, as discussed above, a simple two-state picture of trp-cage, as either folded or unfolded, does not accurately describe its behavior in our simulations. Adding BPTI crowders promotes partially folded forms of trp-cage, via attractive interactions, which leads to the observed reduction in RMSD at intermediate temperatures.

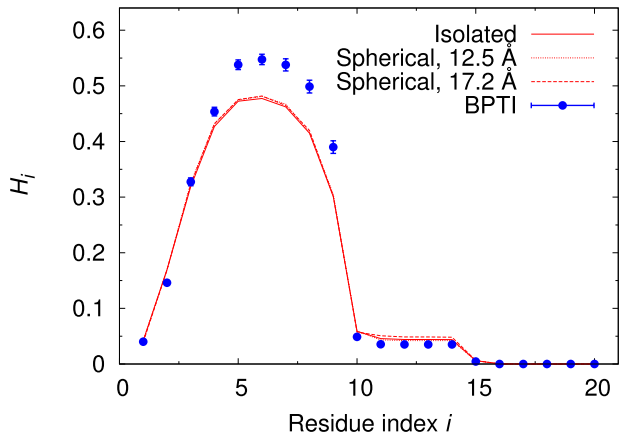

FIG. 3. Residue-specific α-helix probabilities, H_i, for trp-cage at 316 K, as obtained without crowders (red line) and with small spherical (red dots), large spherical (red dashes), and BPTI crowders (blue symbols), using STRIDE[54] secondary-structure assignments. The curves for the systems without crowders and with small or large spherical crowders are almost indistinguishable. For these systems, the statistical uncertainties are small and, for clarity, omitted.

So far, our analysis focused on average properties. It is instructive to also investigate the probability distributions of relevant properties, in order to elucidate how the free-energy landscape of trp-cage is altered by the crowders. Three key folding coordinates are the helix content, H, the radius of gyration, R_g, and the end-to-end distance, R_{ee}, the latter of which is correlated with the opening angle between the N- and C-terminal parts analyzed by Predeus *et al.*[44] The left panel of Fig. 4 shows the joint probability distribution of R_{ee} and H, as obtained for the isolated trp-cage and with BPTI crowders present, at 316 K. In both cases, trp-cage samples two distinct sub-ensembles, one consisting of conformations with helix content $H > 0.2$ and the other comprising coil-like conformations with low H. Upon the addition of BPTI crowders, both sub-ensembles get shifted toward higher R_{ee}, indicating that both types of conformations interact with the crowders. The crowder interaction nevertheless favors

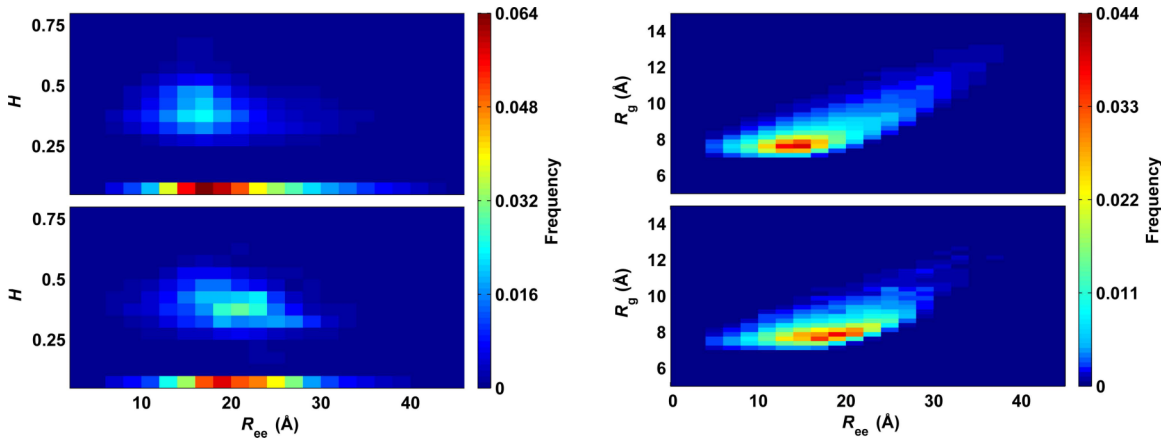

FIG. 4. Conformational ensembles sampled by trp-cage in our simulations, at 316 K. Upper panels are for trp-cage in isolation, and lower panels are for trp-cage in the presence of BPTI crowders. (Left) Joint probability distribution of end-to-end distance, R_{ee}, and helix content, H. (Right) Joint probability distribution of end-to-end distance, R_{ee}, and radius of gyration, R_g.

This article is copyrighted as indicated in the article. Reuse of AIP content is subject to the terms at: http://scitation.aip.org/termsconditions. Downloaded to IP: 130.235.184.47 On: Tue, 08 Dec 2015 22:06:58

helix-containing over coil-like conformations, as manifested by a shift in the relative weight of the two sub-ensembles. The joint (R_{ee}, R_g) distribution is, by contrast, essentially unimodal, both with and without crowders (Fig. 4, right panel). The main effect caused by the crowders is a shift of the peak toward higher R_{ee}. Predeus *et al.* identified, in their simulations with GB1 crowders, a few distinct clusters of non-native trp-cage conformations, stabilized by interactions with the crowders.[44] This kind of sub-structure is not observed in our simulations, which in part may reflect a dependence on the crowder sequence. Similarities and differences between our BPTI results and the GB1 results of Predeus *et al.* are further discussed in Sec. IV.

B. Modes of intermolecular interaction in the trp-cage–BPTI system

The above analysis suggests that the interaction with surrounding BPTI molecules is sufficiently strong to cause significant changes in the conformational ensemble sampled by trp-cage. A snapshot from the simulations, illustrating how trp-cage may interact with the BPTIs, can be found in Fig. 5. To quantitatively analyze the trp-cage–BPTI interaction, it is useful to construct intermolecular residue-pair contact maps, as described in Sec. II. Fig. 6 shows our calculated trp-cage–BPTI contact map at 316 K, which is the same temperature as in Figs. 3 and 4. The contact map immediately shows that the trp-cage–BPTI interaction is not random; instead, a few key residues can be identified. The most interaction-prone residues are Pro12, Pro17, Pro18, and Pro19 in trp-cage and Pro8, Pro9, and Asn24 in BPTI. These residues are located near each other in the respective native structures, so there is one interaction hotspot region on each protein. Among the key residues are all four prolines in trp-cage and two of four prolines in BPTI (Fig. 1). This over-representation of proline is striking but not entirely surprising. In fact, proline is known to be an important player in protein-protein interactions.[55] This property stems in large part from its unique geometry, in combination with its hydrophobic character. The geometry of proline leads to a low propensity for incorporation into α-helices or β-sheets, and thereby an elevated probability of being located at exposed positions in folded structures. In addition, the limited flexibility of proline implies a reduced entropic cost upon binding.

In trp-cage, the proline-segment 17–19, near the C-terminal end, seems ideally positioned to interact intermolecularly (Fig. 1), as it also does in our simulations (Fig. 6). The N-terminal α-helix region is, by contrast, only rarely involved in any contacts with BPTI residues. The observed BPTI-induced stabilization of the α-helix (Fig. 3) is therefore not a result of direct interactions between BPTI residues and this part of trp-cage, but rather an indirect effect. Apparently, the anchoring of the C-terminal tail to BPTI molecules promotes the formation of the α-helix. At the same time, this anchoring prevents a tight packing of the α-helix against the C-terminal tail, as shown by the data for R_{ee} (Fig. 2). As a result, in the presence of the BPTI crowders, trp-cage fails to adopt its global native fold, despite a stabilization of its main secondary-structure element.

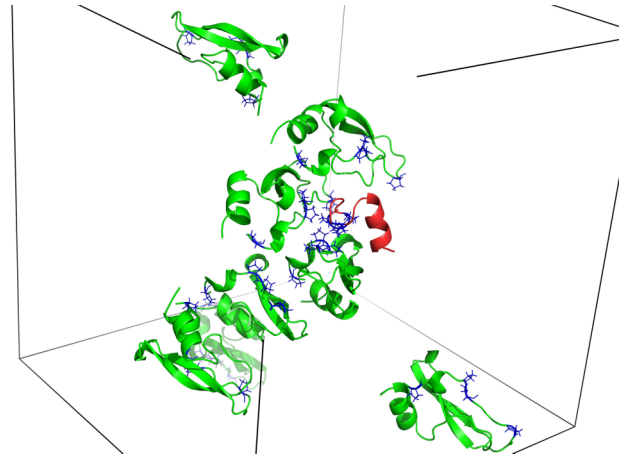

FIG. 5. Snapshot from the trp-cage–BPTI simulations, with the trp-cage molecule in red and the eight BPTIs in green. Proline residues are in blue. The proline-containing C-terminal part of trp-cage interacts with two crowder molecules. The lines indicate the size of the simulation box.

The interaction among BPTI crowders can be analyzed in the same way. The left panel of Fig. 7 shows BPTI-BPTI residue-pair contact frequencies in the trp-cage–BPTI system, again at 316 K. On average, there are fewer BPTI-BPTI than trp-cage–BPTI contacts. By summing up contact map entries, one finds that, at 316 K, trp-cage is involved in an average of 5.4 residue-pair contacts with the eight surrounding BPTIs ($\sum_{ij} n_{ij}^{tc}$), whereas the average number of contacts that a given BPTI forms with other BPTIs is 1.5 ($\sum_{ij} n_{ij}^{cc}/8$). The higher interaction propensity of trp-cage might, at least in part, be due to its more flexible structure. The number of BPTI molecules that the trp-cage molecule interacts with at the same time is typically one or two. More precisely, if we define a given BPTI molecule to be in contact with trp-cage whenever there is at least one residue-pair contact between them, then the probabilities of observing 0, 1, 2, 3, and >3 BPTIs in contact with trp-cage are 5%, 63%, 25%, 6%, and <1%, respectively (at 316 K).

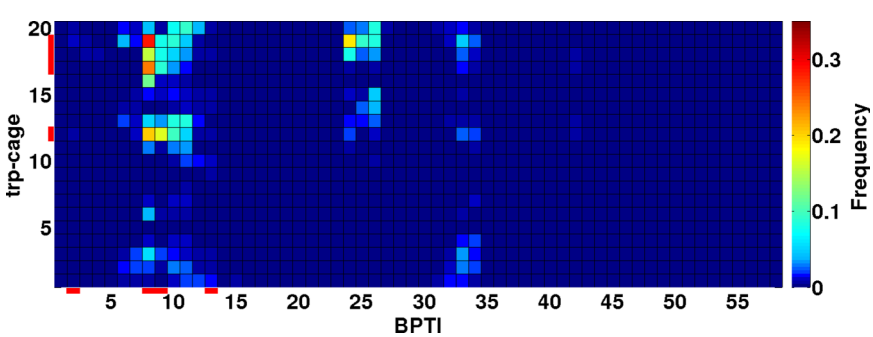

FIG. 6. Trp-cage–BPTI residue-pair contact map, at 316 K. For each pair (i, j), the average number of C^{α}-C^{α} contacts between residue i in trp-cage and residue j in any of the eight BPTI molecules (n_{ij}^{tc}) is indicated. Red bars indicate proline positions in the trp-cage and BPTI sequences.

This article is copyrighted as indicated in the article. Reuse of AIP content is subject to the terms at: http://scitation.aip.org/termsconditions. Downloaded to IP: 130.235.184.47 On: Tue, 08 Dec 2015 22:06:58

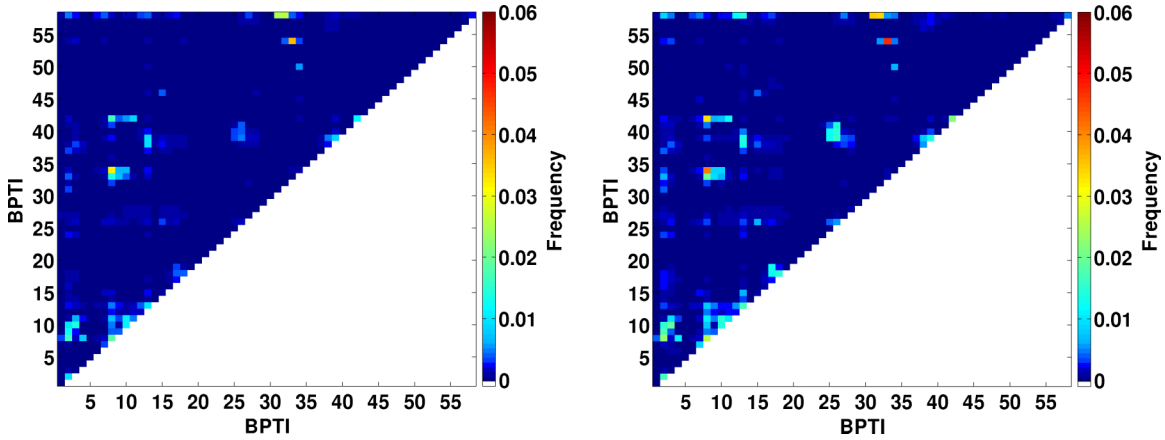

FIG. 7. Intermolecular BPTI-BPTI residue-pair contact maps, at 316 K. For each pair (i, j), the average number of C^{α}-C^{α} contacts between residue i in a given BPTI and residue j in any of the other seven BPTIs (n_{ij}^{cc}) is indicated. Left panel is for the trp-cage–BPTI system. Right panel is from simulations without the trp-cage molecule, under otherwise identical conditions. Note that the color scale is different than in Fig. 6.

For comparison, a self-crowding simulation, without the trp-cage molecule, was carried out as well, under otherwise identical conditions (Fig. 7, right panel). In the absence of trp-cage, the average number of contacts between a given BPTI and other BPTIs increased from 1.5 to 2.4. In part, this difference can be linked to residue Pro8 of BPTI, which is important in both the trp-cage–BPTI and BPTI-BPTI interactions (Fig. 7). In the self-crowding system, there is no competition between trp-cage and BPTI molecules for this interaction site.

IV. DISCUSSION

While a great deal is known about the effects of steric crowders on folded and disordered proteins,[1,37] increasing efforts are now being directed toward studying proteins in more cell-like environments with bio-macromolecular crowding agents. These studies have, in particular, shown that crowding can cause an either upward or downward shift in the stability of folded test proteins,[7–9,11–16] and the direction of the shift can, in part, be rationalized based on net-charge considerations.[9] The protein of the present study, trp-cage, has a well-defined folded structure but is small and malleable. In the previous work by Predeus *et al.*,[44] this protein was studied in the presence of protein GB1 crowders by molecular dynamics simulations, at a temperature where it is folded under dilute conditions. In these simulations, trp-cage sampled not only native-like states but also partially folded states that were not observed in corresponding simulations without crowders. In particular, this study thus suggests that the effect of macromolecular crowding on trp-cage may not be limited to a stability shift, but also involves essential conformational changes.

In this paper, we have used MC-based replica-exchange simulations to explore the equilibrium properties of a system of one trp-cage molecule and eight BPTI crowders, enclosed in a periodic box, over a wide range of temperatures. At low temperatures, we find that trp-cage is prevented from adopting its native fold by competing interactions with the BPTI crowders, which is in line with the results obtained by Predeus *et al.* using protein GB1 crowders.[44] However, when it comes to the precise nature of the destabilizing trp-cage–crowder interactions, our findings differ from those of Predeus *et al.* In the trp-cage–BPTI system, we observe specific binding interactions involving a limited set of key residues (Fig. 6), most of which are prolines. By contrast, Predeus *et al.* found the trp-cage–protein GB1 interactions to be mostly generic. In part, this difference may stem from the different net charges of BPTI (+6) and protein GB1 (−4). As trp-cage carries a positive net charge (+1), this leads to more possible attractive electrostatic residue-pair interactions between trp-cage and protein GB1 than between trp-cage and BPTI, which should indeed make the trp-cage–crowder interactions less specific in the protein GB1 case. In addition, whereas we find two prolines in BPTI to be key residues for the interaction with trp-cage, there are no prolines in protein GB1. Hence, there are at least two reasons to expect the trp-cage–BPTI and trp-cage–protein GB1 interactions to be different in nature.

The robustness of our conclusion that proline residues play a key role in the trp-cage–BPTI interaction is difficult to assess. We note, however, that this role for proline in part stems from its unique geometry, which makes the conclusion less sensitive to uncertainties in energy parameters. Furthermore, it is well known that proline, in large part due to its special conformational properties, is an important amino acid in protein-protein interactions.[55]

While distorting the native fold of trp-cage at low temperatures, we find that the interactions with BPTI crowders give rise to a reduced RMSD at intermediate temperatures. This effect can be linked to a stabilization of the main secondary-structure element, the α-helix, upon anchoring of the proline-rich C-terminal part to BPTI molecules. Closer analysis of the simulated ensembles at intermediate temperatures shows that they can be split into two distinct sub-ensembles, with helix-containing and coil-like conformations, respectively (Fig. 4). These two sub-ensembles are observed both with and without crowders, indicating that the trp-cage–crowder association in part occurs through a conformational-selection mechanism. The association leads to an increase in the relative population of helix-containing conformations. In addition, the crowders have the effect of slightly shifting both sub-ensembles, toward higher end-to-end-distance, which suggests that the trp-cage–crowder association involves an induced-fit mechanism

This article is copyrighted as indicated in the article. Reuse of AIP content is subject to the terms at: http://scitation.aip.org/termsconditions. Downloaded to IP: 130.235.184.47 On: Tue, 08 Dec 2015 22:06:58

as well. To further characterize the trp-cage–crowder interaction, it would be interesting to study the kinetics of the association process, but this is beyond the scope of the present article.

The effects of hard-sphere crowders on the folding thermodynamics of trp-cage have previously been studied by Tsao and Dokholyan.[35] Our results are broadly consistent with theirs, but a direct comparison is difficult to make because the crowders are larger and fewer in our simulations.

The test and crowder proteins used in this article, trp-cage and BPTI, were in part selected for computational tractability. We are not aware of any available experimental data on this system to compare with. Experimental data on simple systems like this could be extremely useful in the development and testing of novel computational methods for crowding simulations.

The trp-cage–protein GB1 system studied by Predeus *et al.*[44] is similar in size to the trp-cage–BPTI system studied here and was simulated using a coarse-grained representation of protein GB1. It is worth noting that we have used an all-atom representation of BPTI. By turning to a suitable coarse-grained description of crowders, it should be possible to extend our calculations to larger systems.

ACKNOWLEDGMENTS

We thank Sigurður Æ. Jónsson for discussions and computational assistance. This work was in part supported by the Swedish Research Council (Grant No. 621-2014-4522). The simulations were performed on resources provided by the Swedish National Infrastructure for Computing (SNIC) at LUNARC, Lund University.

[1]H.-X. Zhou, G. Rivas, and A. P. Minton, Annu. Rev. Biophys. **37**, 375 (2008).
[2]M. Feig and Y. Sugita, J. Mol. Graphics Modell. **45**, 144 (2013).
[3]H.-X. Zhou, FEBS Lett. **587**, 1053 (2013).
[4]F.-X. Theillet, A. Binolfi, T. Frembgen-Kesner, K. Hingorani, M. Sarkar, C. Kyne, C. Li, P. B. Crowley, L. Gierasch, G. J. Pielak, A. H. Elcock, A. Gershenson, and P. Selenko, Chem. Rev. **114**, 6661 (2014).
[5]I. Kuznetsova, B. Zaslavsky, L. Breydo, K. Turoverov, and V. Uversky, Molecules **20**, 1377 (2015).
[6]L. Stagg, S. Q. Zhang, M. S. Cheung, and P. Wittung-Stafshede, Proc. Natl. Acad. Sci. U. S. A. **104**, 18976 (2007).
[7]A. C. Miklos, M. Sarkar, Y. Wang, and G. J. Pielak, J. Am. Chem. Soc. **133**, 7116 (2011).
[8]R. Harada, N. Tochio, T. Kigawa, Y. Sugita, and M. Feig, J. Am. Chem. Soc. **135**, 3696 (2013).
[9]W. B. Monteith and G. J. Pielak, Proc. Natl. Acad. Sci. U. S. A. **111**, 11335 (2014).
[10]D. P. Goldenberg and B. Argyle, Biophys. J. **106**, 905 (2014).
[11]S. Ghaemmaghami and T. G. Oas, Nat. Struct. Mol. Biol. **8**, 879 (2001).
[12]Z. Ignatova, B. Krishnan, J. P. Bombardier, A. M. C. Marcelino, J. Hong, and L. M. Gierasch, Biopolymers **88**, 157 (2007).
[13]K. Inomata, A. Ohno, H. Tochio, S. Isogai, T. Tenno, I. Nakase, T. Takeuchi, S. Futaki, Y. Ito, H. Hiroaki, and M. Shirakawa, Nature **458**, 106 (2009).
[14]A. P. Schlesinger, Y. Wang, X. Tadeo, O. Millet, and G. J. Pielak, J. Am. Chem. Soc. **133**, 8082 (2011).
[15]J. Danielsson, K. Inomata, S. Murayama, H. Tochio, L. Lang, M. Shirakawa, and M. Oliveberg, J. Am. Chem. Soc. **135**, 10266 (2013).
[16]I. Guzman, H. Gelman, J. Tai, and M. Gruebele, J. Mol. Biol. **426**, 11 (2014).
[17]J. W. Neidigh, R. M. Fesinmeyer, and N. H. Andersen, Nat. Struct. Biol. **9**, 425 (2002).
[18]A. Irbäck and S. Mohanty, J. Comput. Chem. **27**, 1548 (2006).
[19]A. Irbäck, S. Mitternacht, and S. Mohanty, BMC Biophys. **2**, 2 (2009).
[20]L. Qiu, S. A. Pabit, A. E. Roitberg, and S. J. Hagen, J. Am. Chem. Soc. **124**, 12952 (2002).
[21]C. D. Snow, B. Zagrovic, and V. S. Pande, J. Am. Chem. Soc. **124**, 14548 (2002).
[22]J. W. Pitera and W. Swope, Proc. Natl. Acad. Sci. U. S. A. **100**, 7587 (2003).
[23]R. Zhou, Proc. Natl. Acad. Sci. U. S. A. **100**, 13280 (2003).
[24]M. Ota, M. Ikeguchi, and A. Kidera, Proc. Natl. Acad. Sci. U. S. A. **101**, 17658 (2004).
[25]J. Juraszek and P. G. Bolhuis, Proc. Natl. Acad. Sci. U. S. A. **103**, 15859 (2006).
[26]D. Paschek, S. Hempel, and A. E. García, Proc. Natl. Acad. Sci. U. S. A. **105**, 17754 (2008).
[27]R. Day, D. Paschek, and A. E. García, Proteins: Struct., Funct., Bioinf. **78**, 1889 (2010).
[28]M. S. Lee and M. A. Olson, J. Chem. Theory Comput. **6**, 2477 (2010).
[29]J. Heyda, M. Kožíšek, L. Bednárova, G. Thompson, J. Konvalinka, J. Vondrášek, and P. Jungwirth, J. Phys. Chem. B **115**, 8910 (2011).
[30]P. Singh, S. K. Sarkar, and P. Bandyopadhyay, J. Chem. Phys. **141**, 015103 (2014).
[31]Z. A. Levine, S. A. Fischer, J.-E. Shea, and J. Pfaendtner, J. Phys. Chem. B **119**, 10417 (2015).
[32]M. S. Cheung, D. Klimov, and D. Thirumalai, Proc. Natl. Acad. Sci. U. S. A. **102**, 4753 (2005).
[33]D. D. L. Minh, C.-e. Chang, J. Trylska, V. Tozzini, and J. A. McCammon, J. Am. Chem. Soc. **128**, 6006 (2006).
[34]J. Mittal and R. B. Best, Biophys. J. **98**, 315 (2010).
[35]D. Tsao and N. V. Dokholyan, Phys. Chem. Chem. Phys. **12**, 3491 (2010).
[36]A. Samiotakis and M. S. Cheung, J. Chem. Phys. **135**, 175101 (2011).
[37]H. Kang, P. A. Pincus, C. Hyeon, and D. Thirumalai, Phys. Rev. Lett. **114**, 068303 (2015).
[38]B. Macdonald, S. McCarley, S. Noeen, and A. E. van Giessen, J. Phys. Chem. B **119**, 2956 (2015).
[39]S. Qin and H.-X. Zhou, Biophys. J. **97**, 12 (2009).
[40]S. R. McGuffee and A. H. Elcock, PLoS Comput. Biol. **6**, e1000694 (2010).
[41]S. Qin, D. D. L. Minh, J. A. McCammon, and H.-X. Zhou, J. Phys. Chem. Lett. **1**, 107 (2010).
[42]S. Qin, J. Mittal, and H.-X. Zhou, Phys. Biol. **10**, 045001 (2013).
[43]M. Feig and Y. Sugita, J. Phys. Chem. B **116**, 599 (2012).
[44]A. V. Predeus, S. Gul, S. M. Gopal, and M. Feig, J. Phys. Chem. B **116**, 8610 (2012).
[45]A. Irbäck and S. Mitternacht, Proteins **71**, 207 (2008).
[46]S. Mitternacht, I. Staneva, T. Härd, and A. Irbäck, J. Mol. Biol. **410**, 357 (2011).
[47]S. Æ. Jónsson, S. Mohanty, and A. Irbäck, Proteins **80**, 2169 (2012).
[48]S. Mohanty, J. H. Meinke, and O. Zimmermann, Proteins **81**, 1446 (2013).
[49]A. Bille, S. Æ. Jónsson, M. Akke, and A. Irbäck, J. Phys. Chem. B **117**, 9194 (2013).
[50]J. Petrlova, A. Bhattacherjee, W. Boomsma, S. Wallin, J. O. Lagerstedt, and A. Irbäck, Protein Sci. **23**, 1559 (2014).
[51]E. Moses and H.-J. Hinz, J. Mol. Biol. **170**, 765 (1983).
[52]R. H. Swendsen and J. S. Wang, Phys. Rev. Lett. **57**, 2607 (1986).
[53]A. Vendeville, D. Larivière, and E. Fourmentin, FEMS Microbiol. Rev. **35**, 395 (2011).
[54]D. Frishman and P. Argos, Proteins **23**, 566 (1995).
[55]B. K. Kay, M. P. Williamson, and M. Sudol, FASEB J. **14**, 231 (2000).

This article is copyrighted as indicated in the article. Reuse of AIP content is subject to the terms at: http://scitation.aip.org/termsconditions. Downloaded to IP: 130.235.184.47 On: Tue, 08 Dec 2015 22:06:58